Technical Sciences
Academy of Romania
www.jesi.astr.ro

Journal of Engineering Sciences and Innovation
Volume 7, Issue 2 / 2022, pp. 143-158

A. Mechanical Engineering

Received ***10 January 2022*** *Accepted* ***14 June 2022***
Received in revised form ***18 May 2022***

Failure simulation of stratified panel under ballistic impact

GEORGE GHIOCEL OJOC, LARISA TITIRE CHIPER, LORENA DELEANU*

"*Dunărea de Jos*" *University of Galati, Faculty of Science and Environment, 47 Domnească Street, RO-800008, Galati, Romania*

Abstract. This paper presents an analysis of an isothermal model for an impact simulation in order to use the results for virtually optimizing the thickness of the panel for the same threat. The target has a stratified structure; the connection between layers is "bonded", with "breakable" detachment when there is exceeded a value for tensile stress and shear stress, introduced with the value of 90 MPa for tensile loading and 60 MPa for shear stress, these being characteristic values for the resin used for attaching the layers in the actual panel. Using Explicit Dynamics Ansys, it is possible to distinguish the stages of the impact process and how they depend on panel thickness. All bodies involved in impact are deformable, the bullet materials having a Johnson-Cook model and the layer being characterized. Even if the layer material model was simplified to a hardening isotropic bilinear model with data from the literature, the results were validated by the number of layers destroyed for the partially penetrated panels and by the size of the delamination on the back of the last layer. This simulation is useful for reducing the number of initial tests for evaluating the ballistic resistance.

Keywords: FE analysis, stress distribution, impact simulation.

1. Introduction

Ballistic impact is a very complex process and it is difficult to model because failure mechanisms involve different scales, from micro-scale (for fibers that have at least two dimensions in microns) [1] to mezo-scale implying the response of yarns in a fabrics and to macro-scale [2], involving the entire structure or components that have to face the threat [3], [4]. Designers introduce simplifications based on experimental dat, in order to simulate the behavior of the system they are interested in. For instance, a micro-scale simulation [5] could explain how a single

*Correspondence address: lorena.deleanu@ugal.ro

fiber is deformed when it support an impact, but a fabric is difficult to model with all the fibers that contains and specialists take into account the yarns, which are characterized as homogenous bodies (isotropic or not) with associated equivalent mechanical characteristics [6]. The macro-scale simulation considers components of the protection system that have dimensions adequate to computer resources and also equivalent values of the mechanical characteristics for the smallest component the system is composed of. Each level of simulation asks for simplifying hypothesis in order to solve the quest. The model is very particular, it could not be applied to any impact case and these aspect have to be carefully analysed by the designer. In this macro-simulation study, this component is the layer of the composite panel.

Materials under impact have a particular response to dynamic load and the processes need to be modeled: nonlinear response to stress, hardening under stress and stress dependance on strain rate, thermal softening, orthotropic response (for composites), damage by crushing (in the case of ceramics, glass, concrete, rocks), processes involving chemical energy (explosions), failure, phase changes (transition from solid-liquid-gas and vice versa). The modeling of these processes can be done with the help of three components: the state equation, the material strength model and the failure model [2], [7], [8], [9].

In the case of layered composites, laws can be introduced for the evolution of interlaminar tension and yield, such as the cohesive zone model (zero thickness) [10], [11].

The Johnson-Cook model [12], [13] is used for solid materials in general, subjected to high strain rates and high temperatures. The yield strength, Y, varies with strain, strain rate, and temperature:

$$Y = \left[A + B\varepsilon_p^n\right]\left[1 + C\varepsilon_p^*\right][1 - T_H^m] \tag{1}$$

where ε_p is the effective (actual) plastic strain, $\boldsymbol{\varepsilon_p^*}$ is the effective plastic strain rate, T_H is the relative temperature in the Johnson-Cook relation, T_{room} is the ambient temperature, T_{melt} is the melting temperature of the material, A, B, C, n and m being material constants.

In Ansys Explicit Dynamics [14], there are several models for initiating material failure. Any failure model must have two components: crack initiation and post-failure response. Failure due to plastic strain is used for ductile materials. The initiation of failure is based on the plastic strain in the material. If this is greater than a characteristic value (often exeperimentally determined), failure occurs, meaning the material breaks instantly.

The Johnson Cook failure criterion may be used for ductile models of materials subjected to high pressures, high strain rates and high temperature ranges. This failure model is developed in a similar way to Johnson-Cook constitutive model, as a function of stress, strain rate and temperature:

$$D = \sum \frac{\Delta_\varepsilon}{\varepsilon^f} \tag{2}$$

$$\varepsilon^f = \left[D_1 + D_2 e^{D_3\sigma^*}\left[1 + D_4 \ln\left|\dot{\varepsilon}^*\right|\right]\right][1 + D_5 T^*] \tag{3}$$

where ε^f is the strain at break of the material, the first parenthesis reflects the dependence of failure on stress, by the terms D_1, D_2 and D_3; the influence of the strain rate on the failure is introduced by the term D_4, and the last parenthesis quantifies the influence of temperature with the term D_5, and Δ_ε is the variation of the strain for an element.

The material is assumed to be intact until the damage parameter, D, is equal to 1. At this moment, the element crack is initiated and an instantaneous post-failure response is triggered. This model can only be applied to solid bodies [14].

2. The model

For some cases of impact (including bullet – target here modeled), the use of properties without temperature dependence is justified by thermal camera monitoring [6], [15], [16], [17], [18], [19], [20], [21] and the characteristics of materials used for the panels, some of which (such as glass fiber composites), having constant properties over a fairly large temperature range. From the documentary study, the modeling of an impact bullet (9 mm FMJ), with impact velocity of 375 m/s), is analyzed under isothermal conditions. There is a thermal effect, but it is considered weak as compared to the failure mechanisms of the involved solids (breaking, deformation, delamination, friction).

The model consists of the two-body bullet with a "perfectly bonded" jacket-core connection and a panel composed of 8 layers, 10 layers, 12 layers or 16 layers. The real panel, produced and tested [22], has 300 mm x 300 mm, which allowed to execute 3 fires, at a distance between them of 120 mm. Due to running time and hardware resources, only a single hit was simulated on a smaller surface (the model panel area is 120 mm x 120 mm). The bullet was drawn after [23] and in order to reduce the running time, it was positioned as close as possible to the panel, the distance between the tip of the bullet and the plate being 0.258 mm.

The connection between layers is "bonded", with the condition of "breakable" detachment, the detachment of nodes being conditioned by exceeding a value for tensile stress and one for shear stress (90 MPa for tensile loading and 60 MPa for the shear stress), these being characteristic values for the resin used for attaching the layers in the actual panel [22].

For this model, the breakable option was set with "Stress Criteria" [14] and then the connection can be broken during the analysis.

This stress criteria was obtained on the basis of "principle of critical energy" [24], [25]. The breaking takes place if the following condition is true [26]

$$P_T(t) \geq P_{cr}(t) \tag{4}$$

where

$$P_T(t) = \sum_{i=1}^{n} \left(\frac{\sigma_i}{\sigma_{i\,cr}}\right)^{\alpha+1} \tag{5}$$

is the total participation of specific energies time dependent, t, corresponding to stresses σ_i, a dimensionless quantity and it depends on the law of the material behavior,

$$\sigma_i = M_\sigma \varepsilon_i^k \tag{6}$$

where ε_i is the strain (or shear strain), M_σ and k being constants related to material. The exponent α depends on strain rate

$$\alpha = \begin{cases} \frac{1}{k} \; for \; static \; loading \\ \frac{1}{2k} \; for \; rapid \; loading \\ 0 \; for \; shock \; loading \end{cases} \tag{7}$$

$\sigma_{i,cr}$ is the critical value of stress σ_i, meaning the ultimate strength or the stress at break.

The quantity time dependent

$$P_{cr}(t) = 1 - D_T^{(t)} P_{res}(t) \tag{8}$$

is dimensionless and depends on total deterioration $D_T(t)$ and on participation of specific energies of residual stresses, $P_{res}(t)$.

In the case of crackless structure (for which $D_T(t) = 0$) and without residual stresses ($P_{res}(t) = 0$), $P_{cr}(t) = 1$.

For a structure without cracks (generally without deteriorations) and without residual stresses, but shock loaded, relationship (4) becomes

$$\sum_{i=1}^{n} \frac{\sigma_i}{\sigma_{i,cr}} \geq 1 \tag{9}$$

Under normal stress, σ, and shear stress, τ, produced by shock loading ($\alpha = 1$), the structure is broken if

$$\frac{\sigma}{\sigma_{cr}} + \frac{\tau}{\tau_{cr}} \geq 1 \tag{10}$$

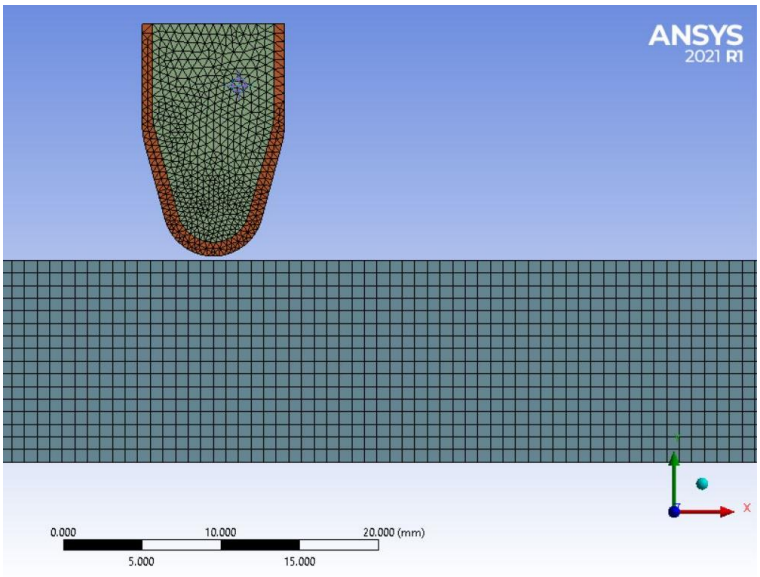

Fig. 1. Detail of mesh network for the proposed model.

The mesh network must be adapted to the particular case that is modeled [6]. For the bullet, a tetrahedral network with at least two elements on the jacket thickness was used, obtained from an initial mesh, over which a mesh with 3 spheres of influence, with a radius of 5 mm, 10 mm and 15 mm, was added in order to have a relatively controlled and smaller growth of network elements. For the 5 mm sphere, the size of the element was 0.35 mm, for the next sphere, it was 0.45 mm and for the largest sphere, 0.55 mm, respectively. Each layer of the panel has a thickness of 0.8 mm (like the layer used to form the composite [22]), with one element per thickness (Fig. 1).

The interaction between bodies is considered with friction, the coefficient of friction being constant, set at 0.1. In any case of impact, the value of friction coefficient is difficult to be measured, the tests reported in the literature being done for relatively lower velocities than those in reality and taking into account only the slip between two bodies. The range found in the literature is from values below 0.1 to 0.4 [27], [28]. In actual impact processes, the friction coefficient is not constant and depends on the pair of invoved materials and the normal stress in the normal.

The model contains a symmetry plane passing through the center of the square panel area and is parallel to one side of the panel (and contains the longitudinal projectile axis).

The initial condition is given by the bullet velocity, considered here v_0 = 375 m/s, also being the measured value for the test campaign.

Boundary conditions involve lateral fixing of the panel. Each layer is fixed on its lateral side surface.

The model is isothermal for two reasons. Explicit Dynamics does not support adiabatic models and the literature has shown that in this area of impact velocities, 100 m/s to 450 m/s, the thermal influence can be neglected in the evaluation of impact failure.

Table 1. Mechanical properties for materials involved in ballistic impact model

Property	**Jacket (brass)**	**Core (Lead alloy)**	**Layer***
Density [kg/m^3]	8450	11350	1904
Specific heat at constant pressure [J (kg ºC]	0.380	128.8	600
Young modulus [MPa]	90000	16000	50000
Tangent modulus, MPa	-	-	10000
Poisson coefficient	0.344	0.44	0.3065
Temperature [°C]	22		
Constants for Johnson-Cook model [12]			
Initial yield limit [MPa]	90	1	550
Hardening constant [MPa]	628	55	
Hardening exponent	0.72	9.8e-002	
Constant for strain rate	0.266	0.231	
Exponentul înmuierii termice	604	221	
Melting temperature [°C]	927	327.5	
Plastic strain rate (/sec)	1	1	
Echivalent plastic strain at break	0.4	0.4	0.09

*hardening biliniar isotropic model after [34]

In these simulations, the Johnson-Cook model was used for the core material (a lead alloy) and the jacket material (a brass alloy), based on the experimental data obtained by [29], [30], [31] and each layer of the panel has the mechanical characteristics in Table 1.
In this model, the layer was considered isotropic as the actual layer is compose of 4 sub-layers with with different orientations of the unidirectional yarns: 0º, 90º, 45º, -45º. The FE model proposed by [32] for "angled fabric panels" (multi-oriented fiber fabrics) point out that these fabrics absorb more energy when are hit by a projectile and the quasi-isotropic response is qualitatively seen on the almost round deformation area and not rhomboidal as for unidirectional fabrics [33].
The ccohesive model zone, with zero thickness (CMZ), was introduced between the layers [35], the name in Explicit Dynamics commands for modeling the resistance of CZM being "Bilinear for interface delamination" (Table 2) [14], the failure criterion being set for “Fracture energies based debonding”, for crack opening mode I.

Table 2. Parameters for modeling the interlaminar delamination

Temperature, °C	22
Maximum normal traction, MPa	70
Normal displacement jump at completion of debonding, mm	5
Maximum tangential traction, MPa	50
Tangential displacement jump at completion of debonding, mm	0.1
Ratio	0.3
Maximum normal contact stress, MPa	100
Critical fracture energy for normal separation, J/m^2	3000
Maximum equivalent tangential contact stress, MPa	-
Critical fracture energy for tangential slip, J/m^2	-
Artificial damping coefficient, s	0.1

3. Results

The results are given for 4 cases of impact, with the same bullet, for v_0 = 375 m/s, the same impact velocity measured for actual test.
The purpose of this analysis is to argue for an intermediate solution on a range of panel thickness. For the range extreme values, the test results were use for validating the model. A lower surface density would be desirable, without affecting the quality of the panel's response to a certain threat.
There are two panel variants experimentally and numerically characterized, with extreme behaviors: 8-layer panel with full penetration (unacceptable in terms of ballistic resistance) and 16-layer panel. This analysis would answer to the following question: there are, in the range of 8…16 layers, a panel that would have a number of layers less than 16, but has the performance that would be worth to be tested in laboratory and, then, as a prototype? It was simulated the impact of the 10- and 12-layer panels, respectively, to see which of them could be a candidate for laboratory-scale fabrication.

Figure 2 presents an example of von Mises stress distiobution on two layers of the panel, in the cross section containing the bullet axis. The absence of stress (zero value) is associated to the layer break as it is visible in Fig. 2a. here, last layer (Fig. 2b) reveal stress peaks due to the bending of the last layer.

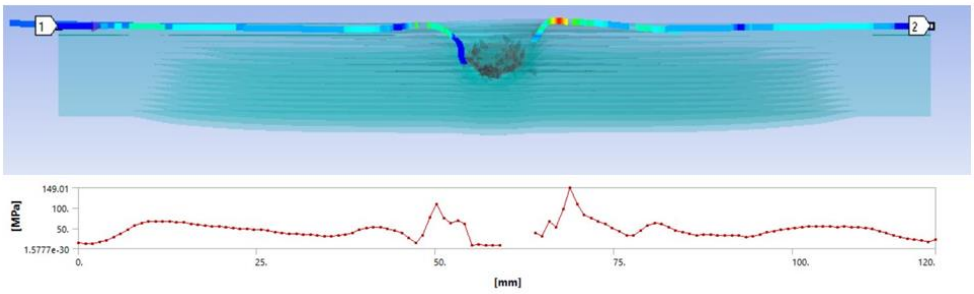

a)

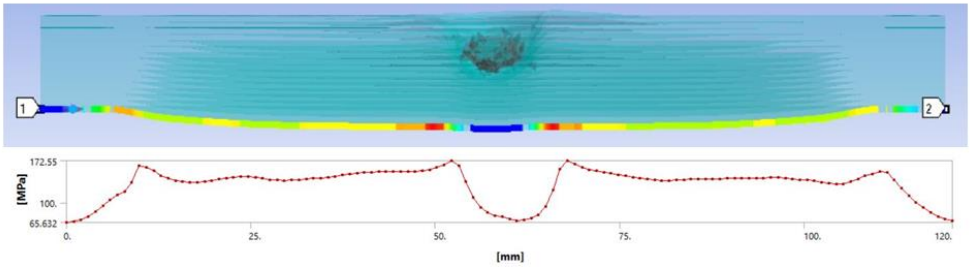

b)

Fig. 2. von Mises stress distribution for a layer: a) first layer (1/16) and b) last layer (16/16), for the panel made of 16 layers, at impact moment $t=1.5\times10^{-4}$ s (end of simulation)

The following figures show, comparatively, at the same time of the simulation, the bullet being transparent in order to better notice the failure mechanisms of panel.
At the first moment of the impact simulation ($t = 7.5\times10^{-6}$ s, fig. 3), the distribution of equivalent stress is similar in the sense of creating local volumes under the bullet, with high stress values. All images point out that the maximum equivalent stress reach high values around the limit at break (around 1400...1500 MPa). Associating the first graph from figure 4, one may notice that layer 1 from 16-layer panel is already broken (stress reached zero value) and layer 1 from 10-layer panel will break as the shape of its stress curve has a lower point near zero. Layer 1 on 8- and 12-panels has high values meaning that break will follow. Initiation of delamination is visible on thicker panels (Fig. 3c and d). All stress distribution are slightly assymetrical due to mesh network. Even in real life this small assymetry could be explained due to the non-homogenity of the fabric and matrix (both dimensions and composition). Also break could occur not on the cross-section that is represented in graph but in another zone of the impacted zone.

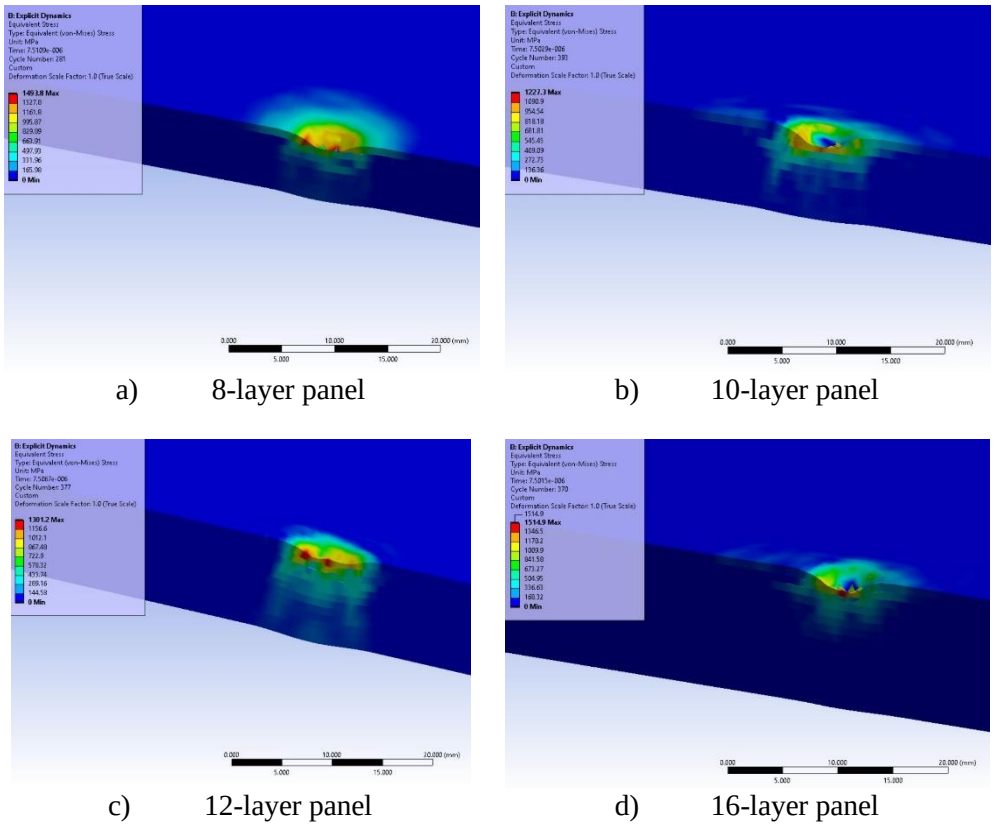

a) 8-layer panel b) 10-layer panel

c) 12-layer panel d) 16-layer panel

Fig. 3. von Mises stress distribution, at moment t=7.5×10^{-6} s,
for panels with different number of layers.

Thicker panels (n = 12 layers and n = 16 layers) have minimum values in the impacted area. Reaching the value of zero (for the panel with n = 16) suggests the break of the layer and values slightly higher than zero (60…70 MPa for the panel with 10 layers) suggest that the moment of break is around the moment of the simulation. For these minimum values, it is possible that the break is not positioned in the plane of symmetry. For the panels with n = 8 layers and n = 12 layers, the equivalent stress values are high, suggesting that the break has not yet occurred in the analyzed cross section.

These values of equivalent stress in graphs for layer 1 noticed better how the first layer behaves (Fig. 3). The length of each layer of the panel model is 120 mm, the value of 60 mm being right the axis of the projectile and coinciding with the impact direction (perpendicular to the panel surface).

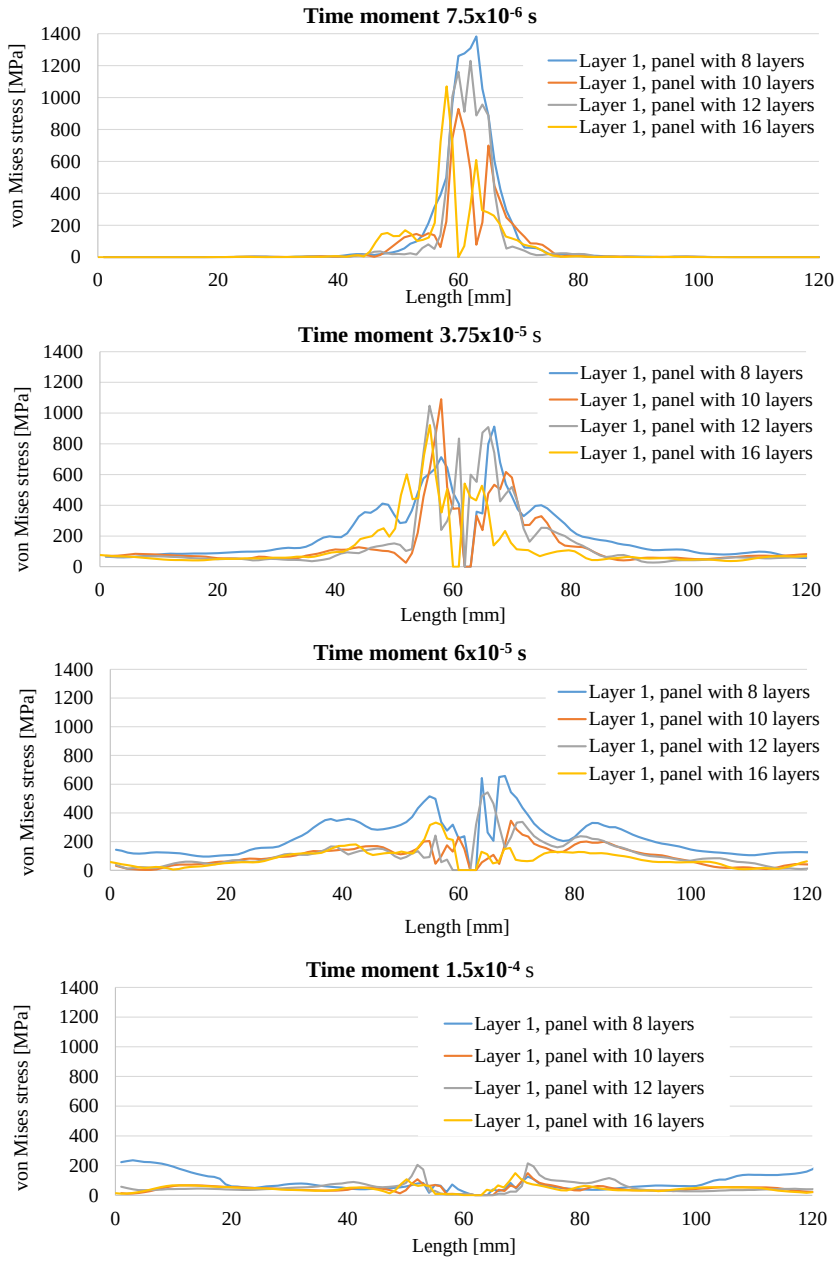

Fig. 3. von Mises stress distribution along layer 1 from each modeled panel, at different moments.

Figure 4 presents evolutions of von Mises stress along the cross section of the last layer several, for consecutive moments during impact. The moments were selected for pointing out the break of the last leyer for the 8-layer panel (that is totally penetrated by the projectile).

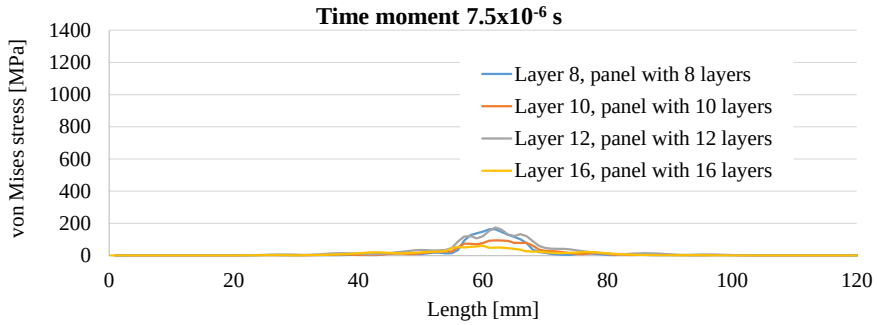
Time moment 7.5x10-6 s
von Mises stress [MPa]
1400
1200
1000
800
600
400
200
0
0
20
40
60
80
100
120
Length [mm]
Layer 8, panel with 8 layers
Layer 10, panel with 10 layers
Layer 12, panel with 12 layers
Layer 16, panel with 16 layers

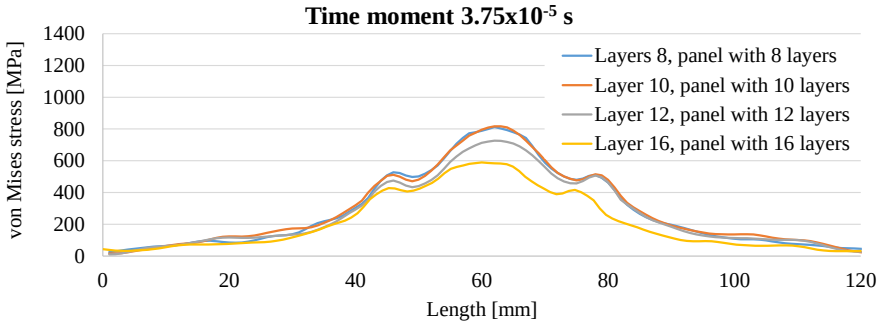
Time moment 3.75x10-5 s
von Mises stress [MPa]
1400
1200
1000
800
600
400
200
0
0
20
40
60
80
100
120
Length [mm]
Layers 8, panel with 8 layers
Layer 10, panel with 10 layers
Layer 12, panel with 12 layers
Layer 16, panel with 16 layers

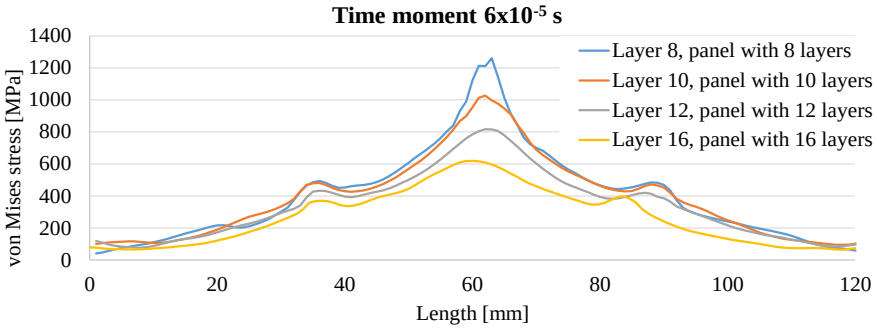
Time moment 6x10-5 s
von Mises stress [MPa]
1400
1200
1000
800
600
400
200
0
0
20
40
60
80
100
120
Length [mm]
Layer 8, panel with 8 layers
Layer 10, panel with 10 layers
Layer 12, panel with 12 layers
Layer 16, panel with 16 layers

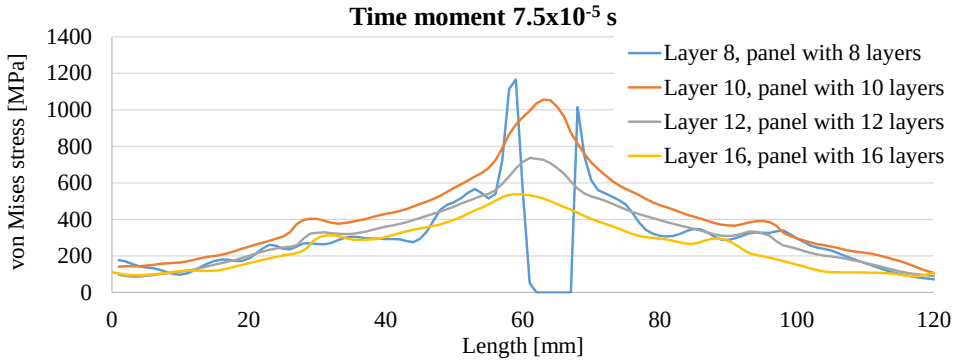
Time moment 7.5x10-5 s
von Mises stress [MPa]
1400
1200
1000
800
600
400
200
0
0
20
40
60
80
100
120
Length [mm]
Layer 8, panel with 8 layers
Layer 10, panel with 10 layers
Layer 12, panel with 12 layers
Layer 16, panel with 16 layers

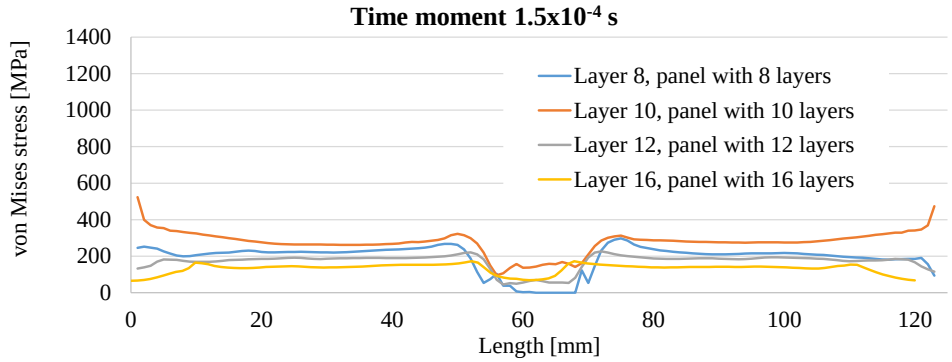

Fig. 4. von Mises stress distributions for the last layer of each panel.

Till t=6×10^{-5} s, the values for von Mises stress increase, for each momen, maximum values being obtained for thinner panels. For the thinnest panel (8-layer panel) this value of more than 1200 MPa suggests that this last layer will be broken after this moment.

At the following moment, t= 7.5×10^{-5} s, the last layer of the 8-layer panel has already been broken and the last layer of the 10-layer panel has the stress curve with a maximum of about 1140 MPa, too close to the limit at break considered for the layer, even if, after this moment, the peak decreases. The last moment of the simulation (t=1.5×10^{-4} s) reveals that impact process will end as the values of von Mises stress decrease under the yield limit, but peaks appear due to bending of broken zones in the impact zone but also near the fixing surface of the layer, bigger for thinner panels.

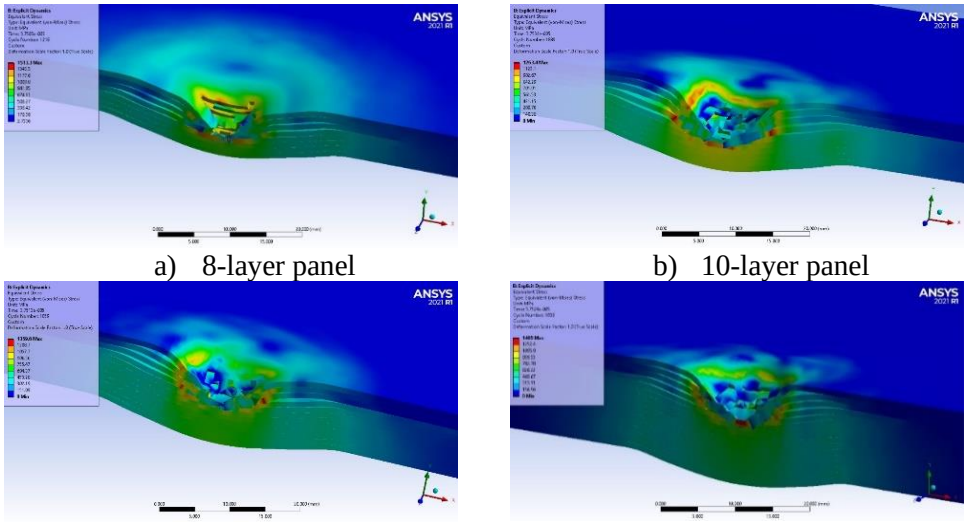

a) 8-layer panel b) 10-layer panel

c) 12-layer panel d) 16-layer panel

Fig. 5. Equivalent stress distributions, at moment t=3.75×10-5 s

At time t=3.75×10^{-5} s, (Fig. 5 and Fig. 4), maximum stress values are at the edge of the contact between the projectile and the panel, except for the panel with n=16 layers. Maximum values exceed the yield strength associated with the layer material (550 MPa). The red micro-zones (maximum values) are either below the projectile or laterally because the projectile presses and pushes the layers laterally. With the exception of the panel with n = 16 layers, the other panels develop maximums of 700…800 MPa. Delamination exists on all panels.

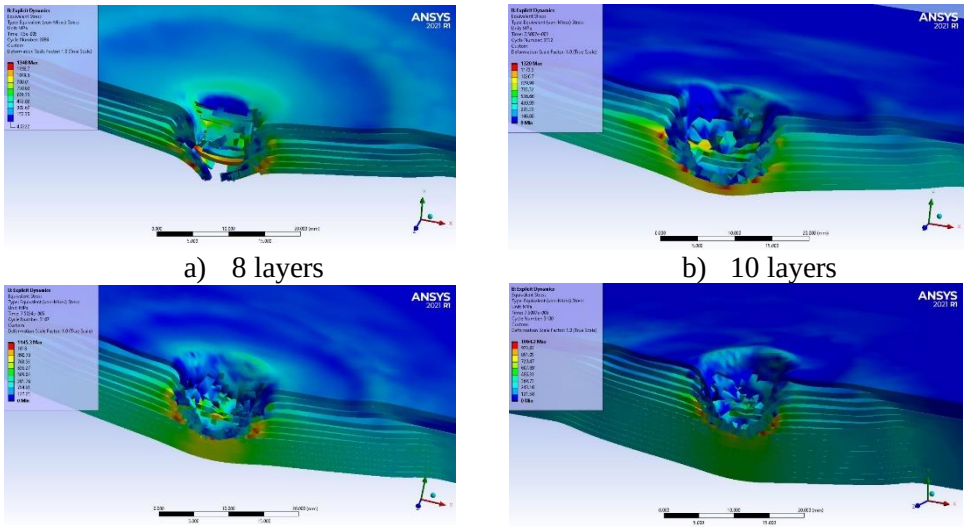

a) 8 layers b) 10 layers

c) 12 layers d) 16 layers

Fig. 5. Equivalent stress distributions, at moment t=7.5×10^{-5} s, impact velocity v_0=375 m/s.

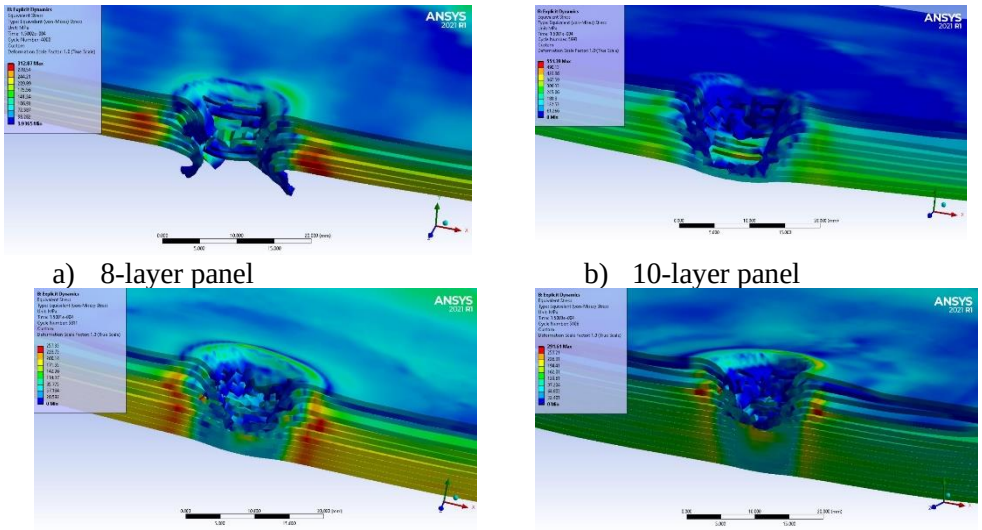

a) 8-layer panel b) 10-layer panel

c) 12-layer panel d) 16-layer panel

Fig. 6. Images from the end of simulation, t=1.5×10-4 s

At the simulation end, the equivalent stress decreased, both on layer 1 and on the last layer (see equivalent stress distribution in the panel cross section Fig. for the equivalent stress distribution along layer 1 and last layer of each panel).

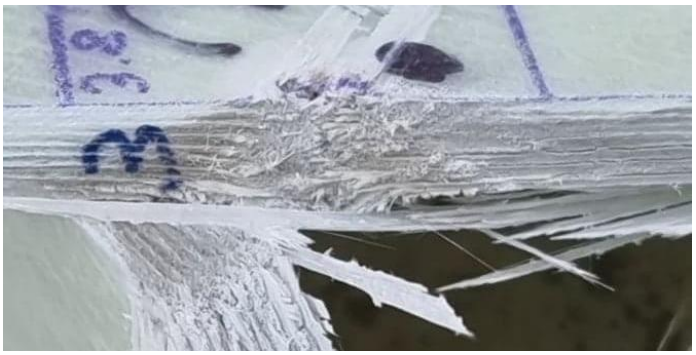

a)

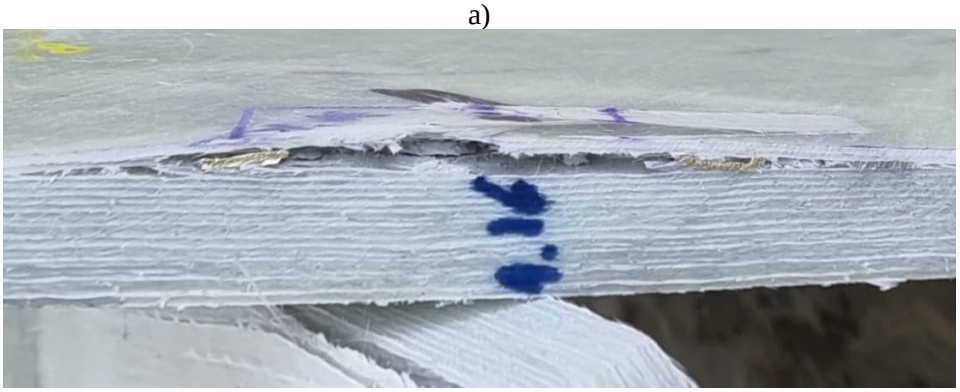

b)

Fig. 7. Photographs of a) 8-layer panel and b) 16-layer panel, after being tested and then cut

If one compare images from simulation (Fig. 6a and d) to actual photos of the tested panels (Fig. 7a and b), they are resembling and the delamination is similar.
Table 5 shows information on delamination size, on tested panels and on simulations. The largest difference, of 29.4% as compared to the value measured on tested panels, was obtained for the 8-layer panel, with total penetration. This difference could have been due to the higher elasticity of the real panel and the fact that, when the bullet passed through the last layers, the separation between them was more severe. For the 16-layer panel, a small difference of 10.1% was obtained between the real one and the simulated panel, acceptable for these macro simulation conditions. The results are reasonably close to use the material model in other simulations, in not very large parameter ranges (for number of layers, impact velocity).

Table 5. Diameters of the delamination circles on the tested panels (on their back face) and on models [22]

Panel	**Panel thickness (average)**	**Diameter 1 fire 1**	**Diameter 2 fire 2**	**Diameter 3 fire 3**	**Average diameter**	**Diameter from the model**
	[mm]					
8 layers	6.37	165	165.9	158.09	**162.99**	**117.04**
16 layers	12.49	105.86	111.5	108.62	**108.66**	**100.19**

4. Conclusions

This paper presented a model for the impact projectile – stratified panel, at macro level, with the following aspects:
- all the involved bodies and materials are in the elasto-plastic field, with EPS failure criterion (equivalent plastic straisn at break); simulations with all bodies being deformable are more realistic,
- delamination modeling,
- identifying the stages for total penetration and partial penetration,
- simulations for the panels tested in the laboratory and the model were validated based on the number of broken layers (± 1 layer) and the delamination size on the back of the panel,
- simulation of cases for intermediate thicknesses between 8 layers and 16 layers because, from the results of laboratory tests, a "reserve" of impact resistance was qualitatively found, in the sense of establishing, at the modeling level, some intermediate effective thicknesses, but smaller, for the same threat,
- running 4 cases at a speed of 375 m/s, velocity that was the average velocity of tests performed in the laboratory [22].

Cases with intermediate thicknesses between panel whole penetration (8 layers) and a panel that proves to face the threat (16 layers) were run; for 10-layer, 12-layer panels, which resulted in a numerical solution that could be validated by testing and provide good ballistic protection, but with a lower surface density (implicitly, panel thickness).

Even if the layer material model was simplified to a hardening isotropic bilinear model with data from the literature, the results were validated by the number of layers destroyed for the partially penetrated panels and by the size of the delamination on the back of the last layer.

This simulation is useful for reducing the number of initial tests for evaluating the ballistic resistance.

References

[1] Sockalingam S., Casem D. T., Weerasooriya T., & Gillespie Jr. J.W., Chapter 9 High Strain Rate Transverse Compression Response of Ballistic Single Fibers. In Kimberley J. et al. (Eds.), *Dynamic Behavior of Materials*, Vol. 1, Conference Proceedings of the Society for Experimental Mechanics Series, 2018.

[2] Meyers M. A., *Dynamic Behavior of Materials*, John Wiley & Sons, Inc., 1994, USA.

[3] Mishnaevsky Jr. L., *Computational Mesomechanics of Composites. Numerical analysis of the effect of microstructures of composites on their strength and damage resistance*, John Wiley and Suns, 2007

[4] Pirvu C., Ionescu T. F., Deleanu L., Badea S., *Simplified simulation of impact bullet - stratified pack for restraining ballistic tests*, MATEC Web Conf., Vol. 112, 2017, 21st Innovative Manufacturing Engineering & Energy International Conference, IManE&E 2017.

[5] Sockalingam S., *Transverse Impact of Ballistic Fibers and Yarns – Fiber Length-Scale Finite Element Modeling and Experiments*, PhD thesis, University of Delaware, 2016, USA.

[6] Grujicic M., Snipes J., Ramaswami S., Avuthu V., *Unit-cell-based derivation of the material models for armor-grade composites with different architectures of ultra-high molecular-weight polyethylene fibers*, International Journal of Structural Integrity, **7**, 4, 2016, p. 458-489.

[7] Donea J., Huerta A., Ponthot,J.-Ph., Rodrıguez-Ferran A., Chapter 14. *Arbitrary Lagrangian–Eulerian Methods. In Stein*, E., de Borst R. & Hughes T. J. R. (Eds.), Encyclopedia of Computational Mechanics, Volume 1: Fundamentals, 2004, John Wiley & Sons, Ltd.

[8] Hosford W. F., *Mechanical Behavior of Materials* (2nd ed.), Cambridge University Press, UK, 2010.

[9] Lee H.-H., *Finite Element Simulations with ANSYS Workbench 2021*, SDC Publications. USA, 2021.

[10] Chowdhury U., Wu X.-F., *Cohesive zone modeling of the elastoplastic and failure behavior of polymer nanoclay composites*, Journal of Composites Science, **5**, 131, 2021.

[11] Joki R. K., Grytten F., Hayman B., Sørensen B. F., *Determination of a cohesive law for delamination modelling - Accounting for variation in crack opening and stress state across the test specimen width*, Composites Science and Technology, **128**, 2016, p. 49-57.

[12] Johnson G. R., Cook W. H., *Fracture characteristics of three metals subjected to various strains, strain rates, temperatures and pressures*, Engineering Fracture Mechanics, **21**, 1985, 31-48.

[13] Schwer L., *Optional Strain-Rate Forms for the Johnson Cook constitutive model and the role of the parameter Epsilon*_01, Dynamore GmbH, LS-Dyna, Andwerderforum, Frankenthal, Impact, 2007.

[14] *** ANSYS Explicit Dynamics Analysis Guide, 2021, ANSYS, Inc., USA

[15] Alonso L., Martínez-Herguetac F., Garcia-Gonzalez D., Navarro García-Castillo C. S. K., Teixeira-Dias F. (2020). *A finite element approach to model high-velocity impact on thin woven GFRP plates*, International Journal of Impact Engineering. 142, 2020, 103593.

[16] Grujicic M., Pandurangan B, Angstadt D. C., Koudela K. L., Cheeseman B. A., *Ballistic-performance optimization of a hybrid carbon-nanotube/E-glass reinforced poly-vinyl-ester-epoxy-matrix composite armor*, Journal of Materials Science, **42**, 2007, p. 5347–5359.

[17] Hamouda A. M. S., Risby M. S., *Modeling ballistic impact. In Bhatnagar A. (ed.), Lightweight Ballistic Composites. Military and Law-Enforcement Applications*, Woodhead Publishing and Maney, CRC Press, Boca Raton, p. 101-126, 2006, USA.

[18] Ma D., Manes A., Campos Amico S., Giglio M., *Ballistic strain-rate-dependent material modelling of glass-fibre woven composite based on the prediction of a meso-heterogeneous approach*, Composite Structures, 216, 2019, p. 187–200.

[19] Múgica J. I., Aretxabaleta L., Ulacia I., Aurrekoetxea J., *Rate-dependent phenomenological model for self-reinforced polymers*, Composites: Part A, 84, 2016, p. 96-102.

[20] Ojoc G. G., Oancea L., Pîrvu C., Sandu S., Deleanu L., *Modeling of impact on multiple layers with unidirectional yarns*, Mechanical Testing and Diagnosis, **8**, 4, 2019, p. 5-15,

[21] Sockalingam S., *Transverse Impact of Ballistic Fibers and Yarns – Fiber Length-Scale Finite Element Modeling and Experiments*, PhD thesis, University of Delaware, 2016, USA.

[22] Ojoc G. G., *A theoretical and experimental study of ballistic protection packages made of glass fibers*, doctoral thesis, Dunărea de Jos" University of Galați, 2022.

[23] Wiśniewski A., Gmitrzuk M., *Validation of numerical model of the Twaron CT709 ballistic fabric*, Proceedings of 27th International Symposium on Ballistics, BALLISTICS 2013, 2, p. 1535-1544.

[24] Jinescu V. V., *Energonica. Noi principii și legi ale naturii și aplicațiile lor*, Editura Semne, Bucharest, 1997.
[25] Jinescu V. V., *Application in Mechanical Engineering of Principle of Critical Energy*, Lambert Academic Publishing, Saarbrücken, Germany, 2015
[26] Jinescu V. V., Nicolof V.–I., Chelu A., Manea S. – E., *Calculation of the local critical state taking into account the deterioration and the residual stresses*, Journal of Engineering Sciences and Inovation, **2**, 3, 2017, p. 9-21.
[27] Meyer C. S., O'Brien D. J., (Gama) Haque B. Z., Gillespie Jr. J. W., *Mesoscale modeling of ballistic impact experiments on a single layer of plain weave composite*, Composites Part B, 235, 2022.
[28] Ingle S., Yerramalli C. S., Guha A., Mishra S., *Effect of material properties on ballistic energy absorption of woven fabrics subjected to different levels of inter-yarn friction*, Composite Structures, 266, 2021.
[29] Børvik T., Dey S., Clausen A.H., 2009 Perforation resistance of five different high-strength steel plates subjected to small-arms projectiles, International Journal of Impact Engineering. 36, 2009.
[30] Peroni L., Scapin M., Fichera C., Manes A., Giglio M., *Mechanical properties at high strain-rate of lead core and brass jacket of a NATO 7.62 mm ball bullet in numerical simulations of ballistic impacts*, Proceedings of DYMAT 2012.
[31] Giglio M., Gilioli A., Manes A., Peroni L., Scapin M., *Investigation about the influence of the mechanical properties of lead*, EPJ Web of Conferences **26**, 04010. 2012.
[32] Wang Y., Chen X., Young R., Kinloch I., Wells G., *A numerical study of ply orientation on ballistic impact resistance of multi-ply fabric panels*, Composites Part B: Engineering, **68**, 2015, p. 259-265.
[33] Patnaik G., Kaushik A., Rajput A., Prakash G., Velmurugan R., *Ballistic performance of quasi-isotropic CFRP laminates under low velocity impact*, Journal of Composite Materials, **55**, 24, p. 3511-3527.
[34] Naresh K., Shankar K., Rao B.S., Velmurugan R., *Effect of high strain rate on glass fiber reinforced epoxy laminated composites*, Composites Part B, **100**, p. 125-135
[35] *** *Cohesive Zone Material (CZM) Model*, Release 18.2 - © ANSYS, Inc. https://www.mm.bme.hu/~gyebro/files/ans_help_v182/ans_thry/thy_mat11.html